

Dynamics of Ising models with damping

J. M. Deutsch

Department of Physics, University of California, Santa Cruz, California 95064, USA

A. Berger

CIC nanoGUNE Consolider, Mikeletegi Pasealekua 56, E-20009 Donostia, Spain

(Received 30 August 2007; published 28 March 2008)

We show for the Ising model that it is possible to construct a discrete time stochastic model analogous to the Langevin equation that incorporates an arbitrary amount of damping. It is shown to give the correct equilibrium statistics and is then used to investigate nonequilibrium phenomena, in particular, magnetic avalanches. The value of damping can greatly alter the shape of hysteresis loops, and for small damping and high disorder, the morphology of large avalanches can be drastically affected. Small damping also alters the size distribution of avalanches at criticality.

DOI: [10.1103/PhysRevB.77.094437](https://doi.org/10.1103/PhysRevB.77.094437)

PACS number(s): 75.40.Mg, 75.60.Ej, 05.45.Jn

I. INTRODUCTION

In many situations, it is useful to discretize continuous degrees of freedom to better understand them, both from a theoretical standpoint and for numerical efficiency. Ising models are perhaps the best examples of this and have been the subject of numerous theoretical and numerical studies. Renormalization group arguments¹ have explained the reason why this discretization gives equilibrium critical properties of many experimental systems, and these kinds of arguments have been extended to understanding their equilibrium dynamics.² For nonequilibrium situations, such as the study of avalanches, such arguments probably also apply to large enough lengths and time scales as well. However, there are many situations where it would be desirable to understand smaller length scales where other factors should become relevant.

This is particularly true with the dynamics of magnetic systems, where damping is often weak in comparison to precessional effects. For studies of smaller scales, it has been necessary to use more time consuming micromagnetic simulations utilizing continuous degrees of freedom, such as the Landau–Lifshitz–Gilbert equations,³ which is a kind of Langevin equation that gives the stochastic evolution of Heisenberg spins,

$$\frac{ds}{dt} = -\mathbf{s} \times (\mathbf{B} - \gamma \mathbf{s} \times \mathbf{B}), \quad (1)$$

where \mathbf{s} is a microscopic magnetic moment, \mathbf{B} is the local effective field, and γ is a damping factor, which measures the relative importance of damping to precession. In real materials, it ranges⁴ from $\gamma=0.01$ to 1. In contrast, the dynamical rules implemented for Ising models are most often “relaxational” so that energy is instantaneously dissipated when a spin flips, as with the Metropolis algorithm.

However, there is a class of “microcanonical” Ising dynamics⁵ that is reviewed in Sec. II where auxiliary degrees of freedom are introduced and all moves conserve the total energy. The other degrees of freedom can be taken to be variables associated with each spin and allowed moves can then change both the state of the spins and the auxiliary

variables. This can be thought of crudely, as a discretized analogy to molecular dynamics, and is also similar to discrete lattice gas models of fluids.^{6,7} These models give the correct equilibrium Ising statistics of large systems and can also be used to understand dynamics in a limit different from the relaxational case.

Real spin systems are intermediate between these two types of behavior and, as mentioned above, are better described by Langevin dynamics. In the context of spins, the question posed and answered here is: How does one formulate a discrete time version of stochastic dynamics that includes damping and gives the correct equilibrium statistics? In Sec. II A, we are able to show that there is a fairly simple method for doing this using a combination of microcanonical dynamics and an elegant procedure that incorporates damping and thermal noise. This procedure differs from that of the Langevin equation in that it requires non-Gaussian noise. Despite this, the noise has surprisingly simple but unusual statistics.

We will show that this procedure gives the correct equilibrium statistics and verify this numerically in Sec. II B by means of simulation for the two dimensional Ising model with different amounts of damping.

Because the value of damping is an important physical parameter in many situations, it is crucial that there is a straightforward way of incorporating its effects in Ising simulations. This is particularly noteworthy as Ising kinetics are a frequently used means of understanding dynamics in many condensed matter systems.

In Sec. III, we will turn to nonequilibrium problems where, using this approach, we can study the effects of damping on a number of interesting properties of systems displaying avalanches and Barkhausen noise.⁸ We first show how to modify the kinetics for this case and then study systems in two and three dimensions. With modest amounts of computer time, we can analyze problems that are out of the reach of micromagnetic simulations and allow us to probe the effects of damping on the properties of avalanches. This is related to a recent work⁹ by the present authors on how the Landau–Lifshitz–Gilbert equation [Eq. (1)] and relaxational dynamics of avalanches¹⁰ are modified at small to intermediate scales by the inclusion of finite damping. With the

present approach, we find new features and modifications of avalanche dynamics. Specifically, we observe that the shape of hysteresis loops can be strongly influenced by the amount of damping. One of the most striking findings is that there exists a parameter regime of high disorder and small damping where system-size avalanches occur, which are made up of a large number of disconnected pieces. We can also analyze the critical properties of avalanches when damping is small and give evidence that there is a crossover length scale, below which avalanches have different critical properties.

II. NONRELAXATIONAL DYNAMICS

We start by considering a model for a magnet with continuous degrees of freedom, such as a Heisenberg model with anisotropy. The Ising approximation simplifies the state of each spin to either up or down, that is, $s_i = \pm 1$, with $i = 1, \dots, N$. One important effect that is ignored by this approximation is that of spin waves that allow the gradual transfer of energy between neighbors and, for small oscillations, give an energy contribution per spin equal to the temperature T (here, we set $k_B = 1$). This motivates the idea that there are extra degrees of freedom associated with every spin that can carry (a positive) energy e_i . Creutz⁵ introduced such degrees of freedom and posited that they could take any number of discrete values. He used these auxiliary variables e_i to construct a cellular automaton, which gives the correct equilibrium statistics for the Ising model in a very efficient way that did not require the generation of random numbers. Thus, we have a Hamiltonian H_{tot} that is the sum of both spin H_{spin} and auxiliary degrees of freedom H_e : $H_{\text{tot}} = H_{\text{spin}} + H_e$. H_{spin} can be a general Ising spin Hamiltonian and $H_e = \sum_i e_i$. In our model, there is a single auxiliary variable e_i associated with each lattice site i that can take on any real value ≥ 0 .

However, for the purposes of trying to model the dynamics of spins, it also makes sense to allow the e_i 's to interact and exchange energy between neighbors. For example, one precessing spin should excite motion in its neighbors. This exchange was formulated in the context of solidification by using a Potts model instead of an Ising model by Conti *et al.*¹¹ but can equally well be used here.

Now, we can formulate a microcanonical algorithm for the Ising model using the following procedure, very similar to Ref. 11.

- (1) We choose a site i at random.
- (2) We randomly pick with equal probability either a spin or an auxiliary degree of freedom, i.e., s_i or e_i .
 - (a) s_i 's: We attempt to move spins (such as the flipping of a single spin). If the energy cost in doing this is $\leq e_i$, we perform the move and decrease e_i accordingly. Otherwise, we reject the move.
 - (b) e_i 's: We pick a nearest neighbor j and repartition the total energy with uniform probability between these two variables. That is, after repartitioning, $e_i' = (e_i + e_j)r$ and $e_j' = (e_i + e_j)(1-r)$, where $0 < r < 1$ is a uniform random variable.

Note that these rules preserve the total energy and the transitions between any two states that have the same probability. Therefore, this will give the correct microcanonical

distribution. For large N , this is, for most purposes,¹² equivalent to the canonical distribution $\propto \exp(-\beta H_{\text{tot}})$. Note that the probability distribution for each variable e_i , $P(e_i) = \beta \exp(-\beta e_i)$ so that the $\langle e_i \rangle = T$. That is, a measurement of the e_i average directly gives the effective temperature of the system.

A. Extension to damping

The question we ask is how to extend this equilibrium simulation method to include damping. In this case, the system is no longer closed and energy is exchanged with an outside heat bath through interaction with the auxiliary variables. As with the Langevin equation, there are two effects. The first is that the energy is damped. We call the dissipation parameter for each step α , which will lie between 0 and 1. Then, at each time step, we lower the energy with $e_i \rightarrow \alpha e_i$ for all sites i . By itself, this clearly will not give a system at finite temperature and we must also include the second effect of a heat bath, which adds energy randomly to the system. In the case of the Langevin equation, a Gaussian noise term $n(t)$ is added to keep the system at finite temperature. A discretized version of this that evolves the energy $e(t)$ at time step t is

$$e(t+1) = \alpha e(t) + n(t). \quad (2)$$

This equation will not work if the noise $n(t)$ is Gaussian as this does not give the Gibbs distribution $P_{eq}(e) = \beta \exp(-\beta e)$. Therefore, we need to modify the statistics of $n(t)$. It is possible to do so if we choose $n(t)$ at each time t from a distribution

$$p(n) = \alpha \delta(n) + (1 - \alpha) \beta e^{-\beta n} \theta(n), \quad (3)$$

where θ is the Heaviside step function. To show this, we write down the corresponding equation for the evolution of the probability distribution for e ,

$$\begin{aligned} P(e', t+1) &= \langle \delta[e' - (\alpha e + n)] \rangle \\ &= \int \int P(e, t) p(n) \delta[e' - (\alpha e + n)] de dn. \end{aligned} \quad (4)$$

We require that the P as $t \rightarrow \infty$ obeys $P(e, t+1) = P(e, t) = P_{eq}(e) = \beta \exp(-\beta e)$ for $e > 0$. It is easily verified that by choosing this form of $P(e, t)$ and by choosing $p(n)$ as in Eq. (3), we satisfy Eq. (4).

Therefore, to add damping to this model, we add the following procedure to the steps stated above:

- (3) Choose a uniform random number $0 < r < 1$. If $r < \alpha$, then $e_i \rightarrow \alpha e_i$. Otherwise, $e_i \rightarrow \alpha e_i - T \ln(r')$, where r' is another uniform random number between 0 and 1.

If we assume that the probability distribution for the total system is of the form $P_{\text{Gibbs}} \propto \exp(-\beta H_{\text{tot}}) = \exp(-\beta H_{\text{spin}}) \exp(-\beta H_e)$, we will now show that steps 1–3 of this algorithm preserve this distribution. By following the same reasoning as above for the microcanonical simulation, moves implementing steps 1 and 2 do not change the total energy, and they preserve the form of P_{Gibbs} because P_{Gibbs} depends only on the total energy (H_{tot}), and steps 1 and 2 explore each state in an energy shell with uniform probabil-

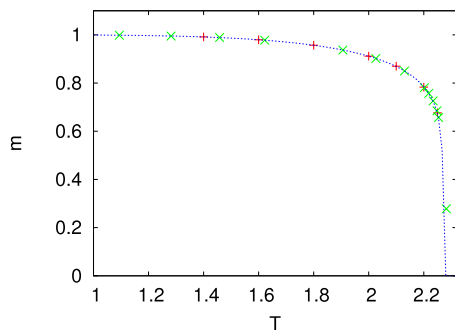


FIG. 1. (Color online) Plot of results obtained for the two-dimensional Ising model on a 128^2 lattice for two different values of the damping parameter. This is a plot of the average magnetization per spin m vs T . The \times 's are for no dissipation, $\alpha=1$, which is a purely microcanonical simulation. The $+$'s are for $\alpha=0.5$. The dashed curve is the exact solution to this model in the thermodynamic limit.

ity. Because of the form of P_{Gibbs} , its dependence on the variable e_i is $\propto \exp(-\beta e_i)$. According to the above argument, after step 3, it will remain unchanged. Therefore, all steps in this algorithm leave P_{Gibbs} unchanged. The algorithm is also ergodic, and therefore, this will converge to the Gibbs distribution¹³ as $t \rightarrow \infty$.

Because each step preserves the Gibbs distribution, the ordering of the steps is not important in preserving equilibrium statistics. For example, we could sweep through the lattice sequentially instead of picking i at random. We could perform step 3 after steps 1 and 2 were performed N times.

The form of this noise [Eq. (3)], although quite unusual, can be qualitatively understood to some extent. For a large damping or a small α , the strength of the δ function becomes small, and the effect is dominated by the second term, which is $\propto \exp(-\beta n)$ (for positive n). Although this is non-Gaussian, n can be thought of as a random amount of positive energy. In the Langevin equation, noise is often added to a velocity degree of freedom. In terms of a velocity, the exponential form that we have obtained would correspond to a Gaussian if this was expressed in terms of a velocity instead. In the limit of a small damping, where α is close to 1, the effect of the noise becomes small because the first term, which is to add no noise, will dominate the distribution. This is in accord with what happens in the Langevin equation where, if dissipation is small, little thermal noise is needed to keep the system at a given temperature.

B. Equilibrium tests

We performed tests on this algorithm and verified that it did indeed work as expected. We simulated the two dimensional Ising model on a 128^2 lattice with different values of the damping parameter and compared it with the exact results. The average magnetization per spin m is plotted in Fig. 1 as a function of the temperature T and compared to the exact result¹⁴ for large N (dashed curve). The \times 's are the case $\alpha=1$, which is then just an implementation of the microcanonical method¹¹ described above. In this case, the tem-

perature was obtained by measuring $\langle e_i \rangle$ because the energy was fixed at the start of the simulation. The only point that is slightly off the exact solution is in the critical region.¹⁵ The case $\alpha=0.5$ is shown with the $+$'s and lies on the same curve. The results were obtained for $\alpha=0.9$ but are too close to be distinguishable and therefore are not shown.

We also checked that the distribution of auxiliary variables had the correct form. We analyzed the probability distribution for the energy $P(e_i)$ versus energy e_i , which is averaged over all sites i on a linear-logarithmic scale for $\alpha=0.5$. We found that the curves are straight lines over four decades and show the correct slopes. For $T=0.8$, $\langle e_i \rangle = 0.8002$, and for $T=1.1$, $\langle e_i \rangle = 1.1003$.

III. AVALANCHE DYNAMICS

The avalanche dynamics of spin systems have been mainly studied using models that are purely relaxational. There is a whole range of interesting phenomena that have been elucidated by such studies and have yielded very interesting properties. The simplest model that can be used in this context is the random field Ising model with a Hamiltonian,

$$\mathcal{H} = - \sum_{\langle ij \rangle} J s_i s_j - \sum_i h_i s_i - h \sum_i s_i, \quad (5)$$

where J is the strength of the nearest neighbor coupling, h_i is a random field with zero mean, and h is an externally applied field. A magnet is placed in a high field h and then this is very slowly lowered. As this happens, the spins will adjust to the new field by flipping to lower their energy. In the usual situation, the system is taken to be at $T=0$, so that the only moves that lower the energy are accepted. The flipping of one spin can cause a cascade of additional spins to flip, causing the total magnetization M to further decrease. The occurrence of these cascades is called an ‘‘avalanche.’’ At zero temperature, there is one parameter j that characterizes the system, i.e., the ratio of nearest neighbor coupling to the distribution width of the local random fields. When j is small, the system is strongly pinned and will exhibit a number of small avalanches generating a smooth hysteresis loop. For large j , the system will have a system-size avalanche involving most of the spins in the system, leading to a precipitous drop in the hysteresis loop. There is a critical value of j where the distribution of avalanche sizes is a power law and self-similar scaling behavior is observed.

Here, we investigate how this behavior is modified by adding damping to these zero temperature dynamics according to the following rules.

(1) The field is slowly lowered by finding the next field where a spin can flip.

(2) The spins then flip, exchanging energy with auxiliary variables e_i , as described above. The number of times this is attempted is n_m times the total number of spins in the system. Here, we set $n_m=16$. In more detail:

(i) Spin moves: An attempt to move each spin on the lattice is performed by attempting to flip sequentially every third spin in order to minimize artifacts in the dynamics due to updating contiguous spins. (The lattice sites are linearly ordered using ‘‘skew’’ boundary conditions.) Then, all three sublattices are cycled over.

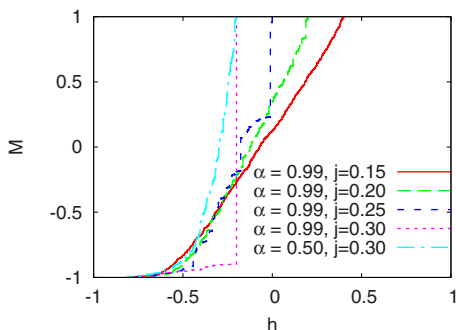


FIG. 2. (Color online) The major branch of the descending hysteresis loop for 64^2 systems using different values of the damping parameter and the spin coupling. Strong damping, $\alpha=0.5$ (dashed-dotted line), is shown in the left most curve as judged from the top of the plot for coupling $j=0.3$, which starts decreasing from $M=1$ at $h=-0.2$, and does not have large abrupt changes. All the other curves are for weak damping, $\alpha=0.99$. In this case but also for $j=0.3$, we see that although M starts to decrease at the same location as for strong damping, it abruptly drops as the field is lowered. As the coupling j is decreased, smooth curves are eventually seen again. Going from left to right, as judged from the top, $j=0.3, 0.25, 0.2$, and 0.15 .

(ii) Energy moves: Exchange of energy with nearest neighbors is performed cycling through all directions of the nearest neighbors. By using the same sequence of updates, the e_i 's exchange energy with their nearest neighbors in one particular direction.

(iii) Dissipation: The energy of each e_i is lowered to αe_i .

(3) We check for when the spins have settled down as follows: if e_i 's are not all below some energy threshold e_{thresh} , set below to be 10^{-4} , or the spin configuration has changed. Step 2 is repeated until these conditions are both met.

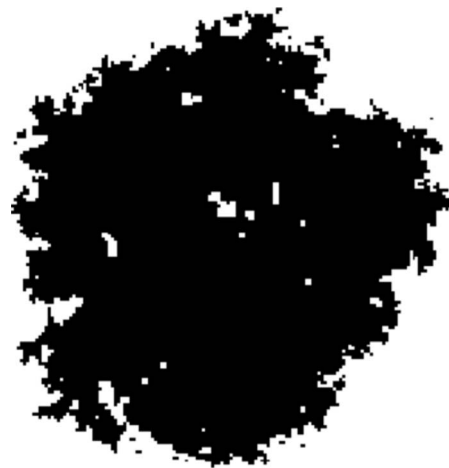
(4) When the spins have settled down, we go back to step 1.

The parameters n_m and e_{thresh} were varied to check that the correct dynamics were obtained. The larger the α , the smaller the dissipation and the larger the number of iterations necessary to achieve the final static configuration at each field.

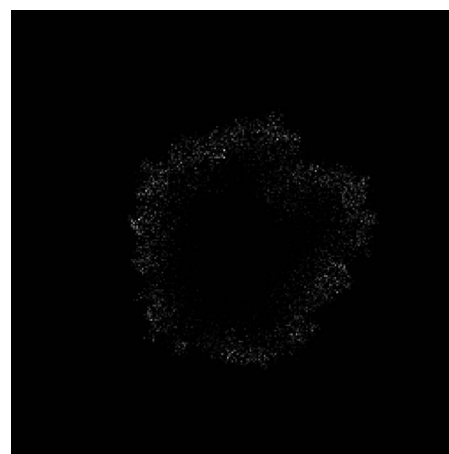
A. Two dimensional patterns

We first investigate the case of two dimensions where it is simpler to visualize the avalanches in various conditions than in three dimensions. Much experimental work and theoretical work on avalanches has been done on two dimensional magnetic films and this case should be highly relevant.¹⁰

We first examine how the hysteresis loops change as a function of the coupling j and the damping parameter α for a 64^2 system. The major downward hysteresis loops are shown in Fig. 2 for a variety of parameters described below. We examine a strong damping, i.e., $\alpha=0.5$. For $j=0.3$, the hysteresis curve is quite smooth with all avalanches much less than the system size (dashed-dotted line). Now, consider the same value of j but with a small damping, $\alpha=0.99$. The curve now is a single downward step with a small tail at



(a)



(b)

FIG. 3. (a) Snapshot of the spin configuration for a 256^2 system with $j=0.35$, $\alpha=0.9$, during a system-size avalanche at the field $h=-0.400007$. (b) A grayscale plot of the auxiliary variables at the same time.

negative h . The lower damping has allowed that system to form a system-size avalanche. The difference is due to the fact that with small damping, the energy of avalanched spins is not immediately dissipated and, as a consequence, heats up neighboring spins, allowing them to more easily avalanche as well. Therefore, a system-size avalanche is seen in the small damping case, leading to the precipitous drop in the hysteresis loop.

When the value of the coupling j is lowered to 0.15 for $\alpha=0.99$, smooth loops are obtained. Figure 2 shows the intermediate values of the coupling parameter as well.

To better understand the reason why the energy of the auxiliary variables can trigger further spins to flip, in Fig. 3 we show the state of a system during a system-size avalanche for $j=0.35$ and a moderately small damping value, $\alpha=0.9$, with $h=-0.400007$. Figure 3(a) shows that the flipped spins form a fairly compact cluster and Fig. 3(b) shows the corresponding values of e_i 's in a grayscale plot, which is suitably normalized. It has the appearance of a halo around the growth front of the avalanche. The spins in the growth front have just flipped and so energy there has not

had a chance to diffuse or dissipate, and thus it has a higher spin temperature. The interior is cold because damping has removed energy from the auxiliary degrees of freedom. This higher temperature diffuses into the unflipped region allowing spins to flip by thermal activation.

Because large avalanches are possible for small damping in a parameter range where the relative effect of the random field is much larger, it is of interest to see if avalanches have a different morphology from that of typical large avalanches for high damping systems. Figure 4 shows such spin configurations first at the beginning of the avalanche and further along during propagation when it has reached roughly half the system size, and finally, when it has reached its final configuration and the maximum auxiliary variable value is $<4 \times 10^{-4}$. The morphology of this is very different from what is seen for large avalanches with stronger coupling, as, for example, Fig. 3. At very small fields, in this figure $h = -7 \times 10^{-5}$, surface tension precludes the formation of minority domains, but because disorder is large, there will be many small regions where the local field is much stronger and these will want to form downward oriented (black) domains. There is a finite activation barrier to forming these that can only be overcome at a finite temperature. However, the majority of the spins still strongly disfavor flipping. However, because damping is small, heat has a chance to diffuse through these regions into the favorable regions, allowing disconnected regions to change orientation by thermal activation. Note that we have numerically checked that small damping with strong coupling also leads to compact configurations, so disorder is an essential ingredient in this new morphology.

B. Three dimensions

We first check that as with two dimensions, the value of the damping parameter can have a large effect on the shape of a hysteresis loop. Figure 5 shows the downward branches of the major hysteresis loop when the only parameter that is changed is the damping α . The system is a 32^3 lattice with $j=0.19$. A value for high damping, $\alpha=0.5$, is the upper line. The lower line is for small damping with $\alpha=0.99$.

A more subtle effect of damping is what happens near criticality. In this case, the value of the critical j will depend on the value of α , as is apparent from the results of Fig. 5. At this point, the distribution of avalanche sizes is expected to follow a power law distribution for large sizes. We located this point and examined system properties in this vicinity. Figure 6 shows examples of such runs for 32^3 systems. Figure 6(a) shows a plot of the magnetization per spin M versus the applied field h for $j=0.165$ and $j=0.167$. For larger values of j , the avalanches rapidly become much larger, as seen in Fig. 5, and for smaller values, avalanches all become small. Figure 6(b) shows a plot of the same quantity with relaxational dynamics near criticality. The avalanches take place over a much smaller range in an applied field.

To quantify this difference, we studied the avalanche size distribution exponent that is obtained by calculating the distribution of avalanche sizes over the entire hysteresis loop. This was studied by averaging avalanches of many runs (200

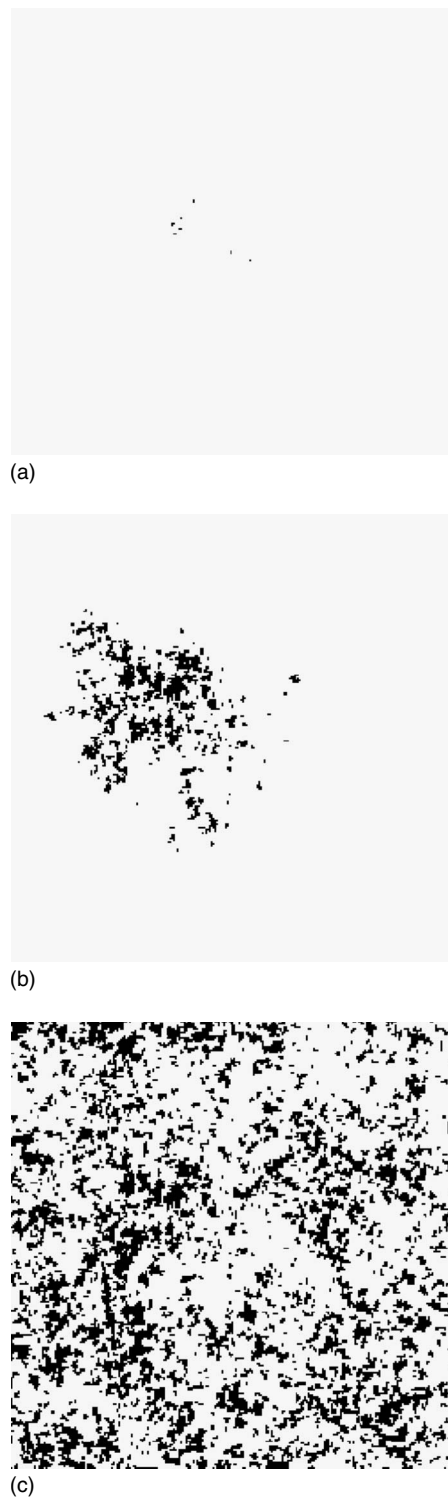


FIG. 4. Snapshots of the spin configurations for a 256^2 system with $j=0.25$, $\alpha=0.99$, during an avalanche at the field $h = -7 \times 10^{-5}$. (a) The beginning of the avalanche. (b) When the avalanche is of order of half the system size. (c) The final configuration of the avalanche.

for $\alpha=0.99$) for 32^3 systems and for different values of parameters. We show a comparison of the avalanche size distribution for $\alpha=0.99$, which is shown with +’s, and for α

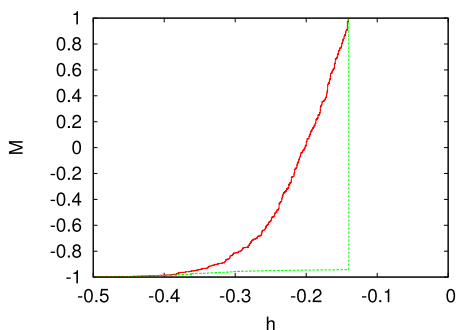


FIG. 5. (Color online) The major branch of the descending hysteresis loops in two 32^3 systems with $j=0.19$ for two different values of the dissipation: upper curve: $\alpha=0.5$ and lower curve: $\alpha=0.99$.

$\alpha=0.9$, which is shown with \times 's in Fig. 7. For $\alpha=0.99$, the curve fits quite well to a power law with an exponent of -1.4 ± 0.1 , as shown in Fig. 7. For purely relaxational dynamics, the same exponent has been carefully measured¹⁶ to be 2.03 ± 0.03 (which is consistent with our results for relaxational dynamics on much smaller systems). With smaller damping, we expect to have a crossover length corresponding to the length scale associated with the damping time, above which the dynamics should appear relaxational. $\alpha=0.9$ appears to show such a crossover from a slope of approximately -1.4 for small avalanches to a higher slope for large ones. A line with a slope of -2 is shown for comparison and appears to be consistent with this interpretation.

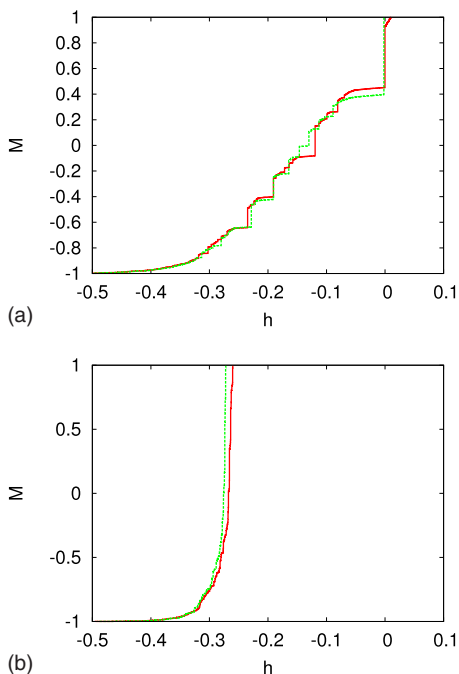


FIG. 6. (Color online) (a) Magnetization versus field for the Ising model with damping described in the text. The system size is 32^3 and the two lines represent two runs close to criticality: one with a coupling of $j=0.165$ and the other of 0.167 . (b) The plot for relaxational dynamics (large damping) with couplings of 0.21 and 0.212 .

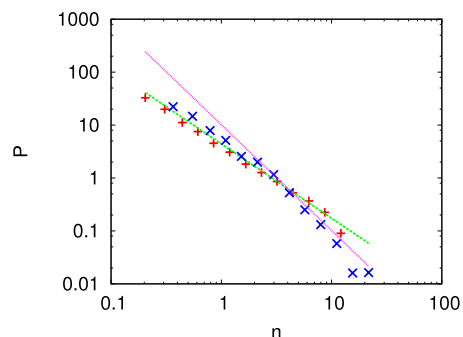


FIG. 7. (Color online) The avalanche size distribution, which is measured for the entire hysteresis loop for $\alpha=0.99$ ($+$) and $\alpha=0.9$ (\times). The x axis is the number of avalanches normalized by its mean size. The y axis is the normalized distribution of sizes. The less negative sloped straight line is a fit of the $\alpha=0.99$ curve and has a slope of -1.4 . The more strongly sloped one has a slope of -2 .

IV. DISCUSSION

This paper has introduced a new set of dynamics for Ising models that incorporates damping in a way that has not before been achieved. The dynamics that has been devised has a lot in common with Langevin dynamics, except for the fact that they are for discrete rather than continuous systems. In Langevin equations, a continuous set of stochastic differential equations are used to model a system. It differs from molecular dynamics in that thermal noise and damping are both added so that the system obeys the correct equilibrium statistics. In the case studied here, we start by considering microcanonical dynamics,^{5,11} which introduces auxiliary degrees of freedom. We then add damping and thermal noise. Whereas the thermal noise is typically Gaussian in the case of the Langevin equation, here it must be taken to be of a special exponential form [Eq. (3)] in order for it to satisfy the correct equilibrium statistics.

The fact that it is possible to model damped systems in this discrete manner should have many useful applications and is easily extended to other kinds of systems, aside from Ising models, especially in applications where computational efficiency is an important criterion.

The case of avalanches in magnetic systems is an interesting nonequilibrium use of these dynamics. Although one might expect that in most situations, for large enough distance and time scales, finite damping will be unimportant, physics at smaller scales is still of great interest, and effects at those scales can propagate to larger scales. Because damping in real materials can be quite small, their effects are readily observable experimentally. This work is expected to be important at intermediate scales. We have investigated the phenomenon seen in this model with varying degrees of damping and found that it makes a qualitative difference to many of the features seen on small and intermediate scales. This work is by no means exhaustive and there are many other effects that can be investigated by straightforward extensions. The effect of dipolar interactions that is in conjunction with damping could also be explored. We have chosen to update the spin and auxiliary variables at equal frequencies.

Varying this should lead to a different value for the heat diffusion coefficient that should change the quantitative values for length and time scales.

It is interesting to compare avalanches in spin systems with those in elastic manifolds^{17,18} where effects of momentum have been considered. An inertial parameter M was introduced to model the effects of momentum locally. If M is small, the depinning transition is continuous and in the same universality class as the relaxational limit. However, for large M , the behavior changes. There is no evidence that in the simulations described here for spin avalanches, the damping parameter is relevant to the long distance, long time behavior. Figure 7 shows a crossover for large sizes to the same power law as that found with relaxational dynamics, at least within the error bars of the simulation.¹⁹ We cannot rule out the possibility that in the regime of small damping and large disorder, as illustrated in two dimensions in Fig. 4 that the situation will be different, but this is hard to simulate in three dimensions for the appropriate system sizes. Work on spin systems, with a conserved order parameter (e.g., the Heisenberg model without disorder), has shown that precessional motion is relevant to the equilibrium dynamic critical behavior²⁰ and this deserves closer scrutiny. It is still possible that if angular momentum was included, which was not done here, it could affect critical properties in a way similar to the above work on elastic manifolds.

The phenomena we have found was in qualitative agreement with earlier work using the Landau–Lifshitz–Gilbert

equations.⁹ As avalanches progress, the effective temperature, which can be quantified by $\langle e_i \rangle$ at site i , will increase as energy is released. This energy then diffuses to the surrounding regions, giving those spins the opportunity to lower their energy by thermal activation. This allows avalanches to more easily progress when the damping is small in contrast to relaxational dynamics, which has effectively infinite damping, $\alpha=0$. This can lead to some substantial differences in avalanche morphology, particularly since for small damping, highly disordered systems can avalanche. At low fields, this leads to a single avalanche, which is composed of many disconnected pieces. Experiments have been devised^{21,22} that are close experimental realization of the two dimensional random field Ising model, and it would be interesting to determine if systems such as this one, or similar to it, show avalanches with this type of morphology.

ACKNOWLEDGMENTS

J.M.D. wishes to thank Peter Young for useful discussions. A.B. would like to acknowledge funding from the Department of Industry, Trade and Tourism of the Basque Government and the Provincial Council of Gipuzkoa under the ETORTEK Program (Project No. IE06-172), as well as from the Spanish Ministry of Science and Education under the Consolider-Ingenio 2010 Program (Project No. CSD2006-53).

-
- ¹S. K. Ma, *Modern Theory of Critical Phenomena*, Frontiers in Physics No. 46 (Perseus Books, Reading, MA, 1976).
- ²B. I. Halperin, P. C. Hohenberg, and S. K. Ma, Phys. Rev. B **10**, 139 (1974).
- ³F. H. de Leeuw, R. van den Doel, and U.ENZ, Rep. Prog. Phys. **43**, 689 (1980).
- ⁴Q. Peng and H. N. Bertram, J. Appl. Phys. **81**, 4384 (1997); A. Lyberatos, G. Ju, R. J. M. van de Veerdonk, and D. Weller, *ibid.* **91**, 2236 (2002).
- ⁵M. Creutz, Ann. Phys. **167**, 62 (1986).
- ⁶U. Frisch, B. Hasslacher, and Y. Pomeau, Phys. Rev. Lett. **56**, 1505 (1986).
- ⁷G. Zanetti, Phys. Rev. A **40**, 1539 (1989).
- ⁸H. Barkhausen, Phys. Z. **20**, 401 (1919); P. J. Cote and L. V. Meisel, Phys. Rev. Lett. **67**, 1334 (1991); J. P. Sethna, K. A. Dahmen, and C. R. Myers, Nature (London) **410**, 242 (2001); B. Alessandro, C. Beatrice, G. Bertotti, and A. Montorsi, J. Appl. Phys. **68**, 2901 (1990); **68**, 2908 (1990); J. S. Urbach, R. C. Madison, and J. T. Markert, Phys. Rev. Lett. **75**, 276 (1995); O. Narayan, *ibid.* **77**, 3855 (1996); S. Zapperi, P. Cizeau, G. Durin, and H. E. Stanley, Phys. Rev. B **58**, 6353 (1998).
- ⁹J. M. Deutsch and A. Berger, Phys. Rev. Lett. **99**, 027207 (2007).
- ¹⁰J. P. Sethna, K. A. Dahmen, and O. Perkovic, in *The Science of Hysteresis II*, edited by G. Bertotti and I. Mayergoyz (Academic, Amsterdam, 2006), pp. 107–179.
- ¹¹M. Conti, U. M. B. Marconi, and A. Crisanti, Europhys. Lett.

- 47**, 338 (1999).
- ¹²M. Lax, Phys. Rev. **97**, 1419 (1955).
- ¹³J. P. Sethna, *Statistical Mechanics Entropy, Order Parameters and Complexity* (Oxford University Press, New York, 2006), p. 170.
- ¹⁴B. M. McCoy and T. T. Wu, *The Two-Dimensional Ising Model* (Harvard University Press, Cambridge, MA, 1973).
- ¹⁵This is to be expected due to the fact that for any finite system there is formally no broken symmetry, which is usually not important for large N due to the exponentially long time it takes to tunnel between energy minima. However, sufficiently close to the critical point this is not the case and the average magnetization does not have a well defined equilibrium value.
- ¹⁶O. Perković, K. A. Dahmen, and J. P. Sethna, Phys. Rev. B **59**, 6106 (1999).
- ¹⁷J. M. Schwarz and D. S. Fisher, Phys. Rev. Lett. **87**, 096107 (2001).
- ¹⁸J. M. Schwarz and D. S. Fisher, Phys. Rev. E **67**, 021603 (2003).
- ¹⁹The point of crossover increases with decreasing damping, but the exact dependence is hard to ascertain given finite size effects.
- ²⁰S. K. Ma and G. F. Mazenko, Phys. Rev. B **11**, 4077 (1975).
- ²¹A. Berger, A. Inomata, J. S. Jiang, J. E. Pearson, and S. D. Bader, Phys. Rev. Lett. **85**, 4176 (2000).
- ²²A. Berger, D. T. Margulies, and H. Do, Appl. Phys. Lett. **85**, 1571 (2004).